STRANGENESS PRODUCTION IN Pb–Pb COLLISIONS AT THE CERN SPS: RESULTS FROM THE WA97 EXPERIMENT

PRESENTED BY L. ŠÁNDOR FOR THE WA97 COLLABORATION:

F. Antinori[j], W. Beusch[f], I.J. Bloodworth[d], R.Caliandro[a], N. Carrer[f], D. Di Bari[a], S. Di Liberto[l], D. Elia[a], D. Evans[d], K. Fanebust[b], F. Fayazzadeh[i], R.A. Fini[a], J. Ftáčnik[g], B. Ghidini[a], G. Grella[m], M. Gulino[e], H. Helstrup[c], M. Henriquez[i], A.K. Holme[i], D. Huss[h], A. Jacholkowski[a], G.T. Jones[d], J.B. Kinson[d], K. Knudson[f], I. Králik[g], V. Lenti[a], R. Lietava[g], R.A. Loconsole[a], G. Løvhøiden[i], V. Manzari[a], M.A. Mazzoni[l], F. Meddi[f], A. Michalon[n], M.E. Michalon-Mentzer[n], M. Morando[j], P.I. Norman[d], B. Pastirčák[g], E. Quercigh[f,j], D. Röhrich[b], G. Romano[m], K. Šafařík[f], L. Šándor[f,g], G. Segato[j], P. Staroba[k], M. Thompson[d], G.D. Torrieri[d], J. Urbán[g], T. Vik[i], O. Villalobos Baillie[d], T. Virgili[m], M.F. Votruba[d], P. Závada[k]

[a] Dipartimento I.A. di Fisica dell'Università e del Politecnico di Bari and Sezione INFN, Bari, Italy
[b] Fysisk institutt, Universitetet i Bergen, Bergen, Norway
[c] Høgskolen i Bergen, Bergen, Norway
[d] School of Physics and Astronomy, University of Birmingham, Birmingham, UK
[e] University of Catania and INFN, Catania, Italy
[f] CERN, European Laboratory for Particle Physics, Geneva, Switzerland
[g] Institute of Experimental Physics, Slovak Academy of Sciences, Košice, Slovakia
[h] GRPHE, Université de Haute Alsace, Mulhouse, France
[i] Fysisk institutt, Universitetet i Oslo, Oslo, Norway
[j] Dipartimento di Fisica dell'Università and Sezione INFN, Padua, Italy
[k] Institute of Physics, Academy of Sciences of the Czech Republic, Prague, Czech Republic
[l] Dipartimento di Fisica dell'Università "La Sapienza" and Sezione INFN, Rome, Italy
[m] Dipartimento di Scienze Fisiche "E.R.Caianiello" dell'Università and Sezione INFN, Salerno, Italy
[n] Institut de Recherches Subatomiques, IN2P3/ULP, Strasbourg, France

The specificity of the WA97 experiment is described. A review of results on the yields and momentum spectra of strange and multi-strange particles and of their centrality dependence is presented. The evidence for the formation of a deconfined state of matter in central Pb–Pb collisions at the SPS energy, provided by these results, is discussed.

1 Introduction

The study of strange particle production in ultra-relativistic nuclear collisions plays an important role in the search for deconfined quark–gluon matter. The strangeness enhancement, i.e. the enhanced relative yield of strange and, in particular, multi-strange particles in central nucleus-nucleus with respect to hadronic interactions, was recognized as one of the sensitive signatures of the transient existence of a quark–gluon plasma (QGP) phase [1,2,3]. These expectations have been fulfilled. Indeed, results from the WA97 experiment, devoted to the study of strangeness production, formed a considerable part of the arguments, allowing CERN to announce in February 2000 a compelling evidence for the existence of a new state of matter [4].

Here we will review the main results from the WA97 experiment, emphasizing the progress achieved since our report at the multiparticle dynamics symposium at Delphi [5].

2 The WA97 experiment

The WA97 experiment, performed at the CERN SPS Omega facility, has been designed for the systematic study of strange and especially multi-strange hyperons and antihyperons at central rapidity in Pb–Pb collisions at a beam momentum of 158 GeV/c per nucleon. The experimental set-up is sketched in Fig. 1. The apparatus, as well as the details of strange particle signal extraction, correction calculations and data analysis are described in [6,7].

The acceptance region of the experiment covers about one rapidity unit centered at midrapidity and transverse momenta higher then a few hundred

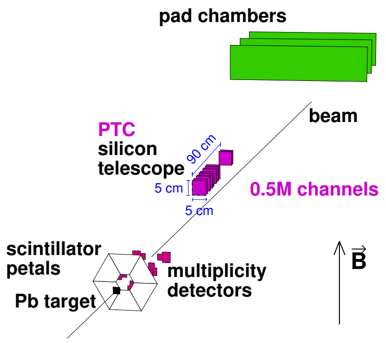

Figure 1. Sketch of the WA97 set-up. The target and all detectors (except for pad chambers) are placed in the 1.8 T uniform field region of the Omega magnet.

MeV/c. An interaction trigger, based on scintillating 'petal' detectors, selects the most central $\sim$ 40% of Pb–Pb collisions. As a reference, p–Be and p–Pb interactions at the same beam momentum are also studied.

In order to cope with the high track density in Pb–Pb collisions, tracking is performed in a high granularity pixel tracking chamber (PTC), based on silicon pixel and microstrip detectors. The K^0_S mesons, the Λ, Ξ^- and Ω^- hyperons and their antiparticles were identified by reconstructing their decays into final states containing only charged particles. A reference sample of negatively charged particles (h^-) has been also analysed. Details of the selection criteria used for the particle identification and for background suppression are discussed in [8]. In the reconstructed strange particle mass spectra (see, e.g. [8]) the mass resolution is better than 6 MeV/c^2 (FWHM).

Two planes of microstrip multiplicity detectors sample the charged particle multiplicity for a study of the centrality dependence of particle yields and spectra. As a measure of centrality we use the average number of wounded nucleons, i.e. nucleons participating in the collision $\langle N_{\rm wound} \rangle$. This is calculated from the measured charged multiplicity in the framework of the wounded nucleon model (WNM). Details of our approach to the centrality measurement are discussed in [9].

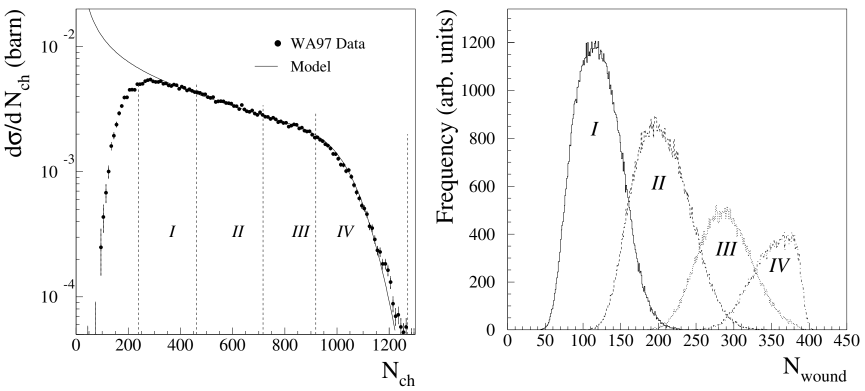

Figure 2. Wounded nucleon model fit to the multiplicity distribution (left panel). Distribution of the number of wounded nucleons in the four multiplicity classes used in data analysis (right panel).

The result of fitting the WNM to the corrected WA97 multiplicity distribution is presented in the left panel of Fig. 2. The four multiplicity classes, used in the centrality analysis, are indicated in the figure by dashed lines. The first multiplicity class is affected by the centrality trigger and the corresponding correction is accounted for. The distribution of the number of wounded nucleons in the four multiplicity bins, obtained from the model, is displayed in the right panel of the figure. The data sample for multiplicity class IV corresponds to the most central $\simeq 3.5\%$ of the total inelastic Pb–Pb cross-section.

3 Results

The main WA97 results concern the transverse mass distributions and the midrapidity yields of strange and multi-strange particles. In addition to the results published in [6,7,10,11], we present the $m_{\rm T}$ distribution and global enhancement for Ω^- and $\overline{\Omega}^+$ separately.

3.1 Transverse mass distributions

The $(y, m_{\rm T})$ distributions of selected particles were parametrized as :

$$\frac{\mathrm{d}^2 N}{\mathrm{d}m_{\rm T}\,\mathrm{d}y} = f(y)\, m_{\rm T}\, \exp\left(-\frac{m_{\rm T}}{T}\right) \tag{1}$$

where $m_{\rm T} = \sqrt{m^2 + p_{\rm T}^2}$ is the transverse mass, assuming the rapidity distribution to be flat in our limited acceptance region ($f(y) = const.$). The inverse slope parameters T have been extracted from the fit of equation (1) to data.

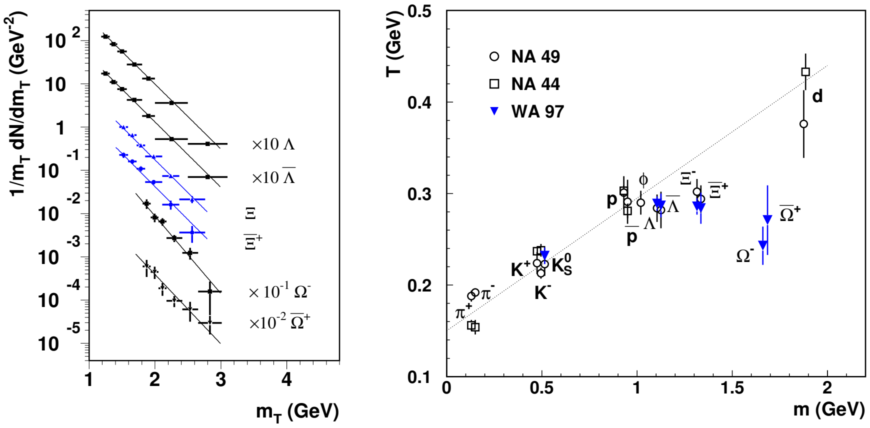

Figure 3. $m_{\rm T}$ spectra of hyperons from Pb–Pb collisions (left panel). Dependence of the $m_{\rm T}$ spectra inverse slopes T on the particle mass m for Pb–Pb collisions at SPS energy (right panel). The line in the right panel represents an approximation of the RQMD model calculations for pions, kaons, protons and deuterons [14].

The m_{T} distributions of hyperons and antihyperons for the Pb–Pb interactions are displayed in the left panel of Fig. 3. It is worth emphasizing the similarity of m_{T} spectra for all particles. As can be seen from the right panel of Fig. 3, where the resulting inverse slopes T are plotted along with results of other SPS experiments, for each species of hyperon the inverse slope for particle and the antiparticle is the same within error limits. This puts a constraint on models predicting different behaviour of antihyperons.

The data on the m_{T} inverse slopes from the NA44, NA49 and WA97 experiments (see [7] and references therein) are displayed in Fig. 3 as a function of the particle mass. The inverse slopes T of non-strange and singly-strange particles exhibit a linear increase with the particle mass. However, the inverse slopes of the Ω and perhaps also the Ξ hyperons deviate significantly from this general trend. In a scenario where a thermal motion is coupled with a transverse collective expansion of the system [12,13] this deviation suggests a rather early freeze-out of multi-strange baryons. This interpretation is supported also by detailed microscopic transport model calculations [14,15]. An alternative scenario assumes a sudden explosive disintegration of the QGP fireball [16,17], implying the same inverse slopes for baryons and antibaryons.

The dependence of the inverse slopes T on the number of participants N_{wound} is shown in fig. 4. Values of T for Λ, $\overline{\Lambda}$, and probably also for Ξ^-, exhibit a slow but steady rise, up to 15% in the centrality range under study ($N_{\mathrm{wound}} > 100$). The inverse slopes of $\mathrm{K}^0_{\mathrm{S}}$, $\overline{\Xi}^+$(not shown here, see [7]) and Ω spectra do not exhibit a significant centrality dependence.

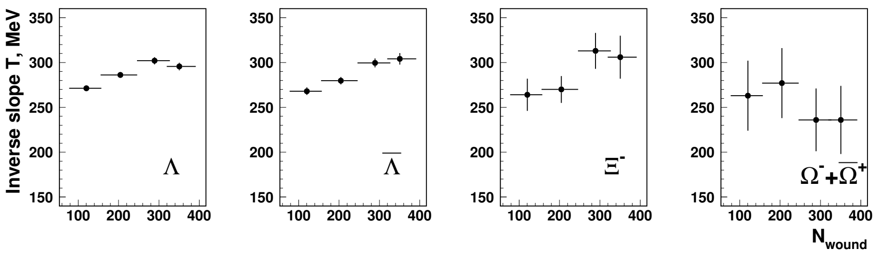

Figure 4. Dependence of m_{T} spectra inverse slopes T on the centrality of collision.

3.2 Particle yields

Integrating formula (1) over one unit of rapidity and extrapolating to $m_{\mathrm{T}} = m$ we get the particle yields :

$$Y = \int_m^\infty \mathrm{d}m_{\mathrm{T}} \int_{y_{\mathrm{cm}}-0.5}^{y_{\mathrm{cm}}+0.5} \frac{\mathrm{d}^2 N}{\mathrm{d}m_{\mathrm{T}}\,\mathrm{d}y}\,\mathrm{d}y \qquad (2)$$

Thermal fits to the calculated particle yield ratios show [18,19] that (multi-) strange baryons and antibaryons are close to chemical equilibrium as expected in a QGP scenario.

The particle yields per participant, calculated according to formula (2) for the four centrality classes of Pb–Pb collisions and normalized to the p–Be yields, are shown in Fig. 5. The data for particles with no quark in common with the incoming nucleons are shown in the right panel, while the others are displayed in the left one. The two groups are kept separate since it is empirically known they can exhibit different production features.

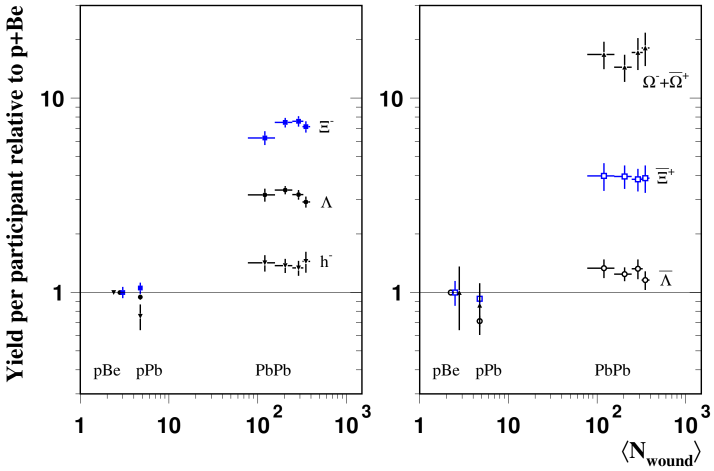

Figure 5. Particle yields per wounded nucleon.

From Fig. 5, one can see that all yields in Pb–Pb collisions are larger than what would be expected from the superposition of elementary nucleon–nucleon interactions (proportionality to the number of wounded nucleons shown by the straight line in the figure). One also notes that, within the covered centrality range, all Pb–Pb normalized yields do not appear to depend on centrality. Therefore, a global enhancement factor E can be computed for $N_{\rm wound} > 100$:

$$E = \left(\frac{Y}{\langle N_{\rm wound} \rangle} \right)_{\rm Pb-Pb} \Bigg/ \left(\frac{Y}{\langle N_{\rm wound} \rangle} \right)_{\rm p-Be} \qquad (3)$$

The resulting values for E are shown in Fig. 6. Within each of the two groups, the global enhancement factor increases with the strangeness content of the particle. The largest effect is observed for the triply strange Ω^- and $\overline{\Omega}^+$, which

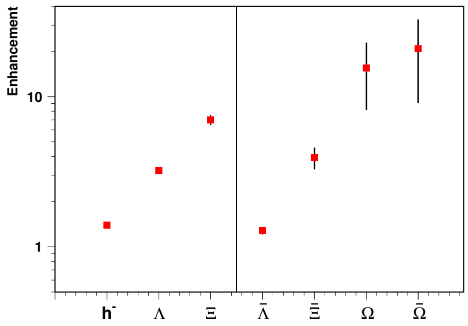

Figure 6. Global strangeness enhancement E.

are enhanced by a factor between 15 and 20. This enhancement pattern is naturally expected in a deconfined scenario, while it is not explained by any known conventional hadronic model [11,20,21] [a].

4 Conclusions

A comprehensive picture of strangeness production in central Pb–Pb collisions is emerging from the results of the WA97 experiment. It can be summarized as follows :

- thermal fits to particle ratios confirm quantitatively the chemical equilibration for all strange baryons and antibaryons at chemical freeze-out,
- enhancement of strange particle production at central rapidity in Pb–Pb with respect to p–Be interactions is observed. It increases with the strangeness content of the particle as expected in a statistical hadronization scenario,
- transverse mass spectra of strange particles demonstrate only week centrality dependence, not exceeding 15% in the centrality range under study ($N_{\rm wound} > 100$),
- the analysis of the $m_{\rm T}$ inverse slopes indicate that multi-strange baryons are decoupled from a hot and dense fireball rather early, either as a result of an early freeze-out or of a sudden hadronization. This puts a stringent constraint on any attempt to explain the enhancement of Ξ and particularly Ω hyperons in terms of hadronic rescattering processes.

[a] At the time of the manuscript preparation an interesting possible explanation has been proposed [22], suggesting that Ω hyperons are produced as topological defects arising from the formation of disoriented chiral condensates.

The ensemble of these features fits naturally into a quark–gluon plasma scenario, while no conventional hadronic microscopic model has succeeded in reproducing them.

References

1. J. Rafelski and B. Müller, *Phys. Rev. Lett.* **48**, 1066 (1982); *Phys. Rev. Lett.* **56**, 2334 (1986) (E).
2. P. Koch, B. Müller and J. Rafelski, *Phys. Rep.* **142**, 167 (1986).
3. P. Koch, B. Müller, H. Stöcker and W. Greiner, *Mod. Phys. Lett.* A **3**, 737 (1988).
4. U. Heinz and M. Jacob, nucl-th/0002042.
5. L. Šándor for the WA97 collaboration in *Proc. of the XXVIII International Symposium on Multiparticle Dynamics (Delphi, Greece, Sept. 1998),* ed. N.G. Antoniou, A.P. Contogouris, F.K. Diakonos, C.N. Ktorides, M. Stassinaki and M. Vassiliou (World Scientific, Singapore, 2000), p. 54.
6. E. Andersen *et al.*, *Phys. Lett.* B **433**, 209 (1998).
7. F. Antinori *et al.*, *Eur. Phys. J.* C **14**, 633 (2000).
8. L. Šándor for the WA97 collaboration, *Nucl. Phys.* B *(Proc. Suppl.)* **71**, 270 (1999).
9. F. Antinori *et al.*, *Eur. Phys. J.* C **18**, 57 (2000).
10. E. Andersen *et al.*, *Phys. Lett.* B **449**, 401 (1999).
11. F. Antinori for the WA97 collaboration, *Nucl. Phys.* A **661**, 130c (1999).
12. K.S. Lee, U. Heinz and E. Schnedermann, *Z. Phys.* C **48**, 525 (1990).
13. U. Heinz, hep-ph/0009170, submitted to *Nucl. Phys.* A
14. H. van Hecke, H. Sorge and Nu Xu, *Phys. Rev. Lett.* **81**, 5764 (1998).
15. A. Dumitru, S.A. Bass, M. Bleicher, H. Stöcker and W. Greiner, *Phys. Lett.* B **460**, 411 (1999)
16. J. Letessier and J. Rafelski, *Int. J. Mod. Phys.* E **9**, 107 (2000).
17. S. Hamieh, J. Letessier and J. Rafelski, *Phys. Rev.* C **62**, 064901 (2000)
18. P. Braun-Munzinger, I. Heppe and J. Stachel, *Phys. Lett.* B **465**, 15 (1999).
19. J. Rafelski and J. Letessier, nucl-th/9902365.
20. F. Antinori *et al.*, *Eur. Phys. J.* C **11**, 79 (1999).
21. S. Soff, S.A.Bass, M. Bleicher, L. Bravina, M. Gorenstein, E. Zabrodin, H. Stöcker and W. Greiner, *Phys. Lett.* B **471**, 89 (1999).
22. J.I. Kapusta and S.M.H. Wong, nucl-th/0012006.